

Programming of Energy Storage System in an Island Microgrid with Photovoltaic and Fuel Cell

Hossein KHORRAMDEL^{1,*}, Benyamin KHORRAMDEL¹ and Marzieh POSHTYAFTEH²

¹*Department of Electrical Engineering, Safashahr Branch, Islamic Azad University, Safashahr, Iran*

²*Department of Electrical Engineering, Dezful Branch, Islamic Azad University, Dezful, Iran*

(* Corresponding author's e-mail: hossein.khorramdel@gmail.com)

Received: 13 February 2014, Revised: 15 May 2014, Accepted: 11 June 2014

Abstract

Photovoltaic (PV) systems in island microgrids (MGs) are becoming increasingly attractive as a means of energy generation, due to new developments in technologies, environmental concerns, and transmission congestion management. Usually, the energy storage system (ESS) is used to store the excess power generated during off-peak hours, and to return it to the system when power from PV is not enough for the system, or generation is more expensive. A real-time dynamic programming algorithm for energy storage in a PV/battery system, based on the battery charge and discharge characteristics, and current and temperature dependence of the capacity of the battery, is presented in this paper. The work aims to extend existing battery-aware programming techniques. It differs from previous works, as it takes into consideration many aspects of battery characteristics that were not considered previously. This allows better use of the battery bank and can prolong the battery service time. This paper also builds a simple PV/battery system in an island microgrid. In this paper, fuel cell power plants (FCPPs) are permanently used to operate in island microgrids, and 2 batteries are used as reserves for charge and discharge in various hours.

Keywords: Energy storage system, microgrid, PV/Battery, renewable energy

Introduction

A microgrid is an active distribution network, which includes both loads and Distributed Generations (DGs) with different reactive power control strategies, and can operate in grid-connected or stand-alone (island) mode [1,2]. It has become increasingly important and necessary to deal with numerous challenges that affect global energy, economics, environment, and security. These challenges have in part resulted from population growth, electric utility restructuring, the production of fossil fuel and its delivery in various parts of the world, environmental pollution, and global warming. These problems present an opportunity for enhancing the structure of generating, transmitting, and delivering reliable and affordable energy [3]. It is envisioned that a portfolio of DG technologies could provide a sizeable fraction of the electricity generation requirements and, in concert with other generation sources, supply reliable energy in a constrained energy infrastructure. DG systems generally consist of the following: small and modular generating systems, such as microturbines, fuel cells, reciprocating engines, cogeneration of heating/power systems, and hybrid units. They use a diversity of fuels, such as hydrogen and natural gas, and renewable energy resources, such as wind, PV, solar, biomass, geothermal, tidal, and hydropower. Electric power, generated by wind turbines, is highly erratic; therefore, the wind energy penetration in electrical power systems can lead to problems related to system operation and the planning of electrical power systems [4]. How to mitigate wind power intermittency, load mismatch, and negative

impacts on grid voltage stability are some key problems to be solved. Solar photovoltaic power is a generic term used for electrical power that is generated from sunlight. A solar photovoltaic system converts sunlight into electricity. The fundamental building block of solar photovoltaic power is the solar cell, or photovoltaic cell. A solar cell is a self-contained electricity-producing device constructed of semiconducting materials. Light strikes on the semiconducting material in the solar cell, creating direct current (DC).

For high energy transfer efficiency, the PV should work at the maximum power point. In the PV system, it is assumed that a maximum power point tracker will be used. In this paper, we focus on an island MG with PV systems with battery energy storage systems (BESSs). With further developments in the PV Systems and lower manufacturing costs, it is envisaged that the PV power will account for a higher percentage of electric power generation in the near future. PV possesses superior characteristics as a pollution free and abundant alternate source of energy with less generation costs [5,6]. However, the maximum power output of PV generally occurs when solar radiation is the strongest, which may not be consistent with the period of system peak loads. To solve the problem of 2 distinct peak periods of a typical system load profile, batteries are installed to store energy forms PV and MG during off-peak periods, and to discharge during evening peak hours. However, the battery should be considered first for safety reasons in practice. In addition, the useful life of the battery, generally less than 4 years, is much shorter than that of the PV arrays. The battery-based charging/discharging scheme can prolong the battery's life. ESS plays a key role in the MG, which is desirable to shave off the peak demand and store the surplus electrical/renewable energy. Sizing of ESS is to be considered first when considering ESS in the MG. Much research works have been done to address this question. BESS is being used in conjunction with renewable energy resources, i.e., wind and solar, where they provide a means of converting these non dispatchable and highly variable resources into dispatchable ones. ESS could also increase the reliability of power systems. The programming algorithm considers many aspects of battery characteristics that were not considered previously [7-10]. The results and analysis will be shown in this paper.

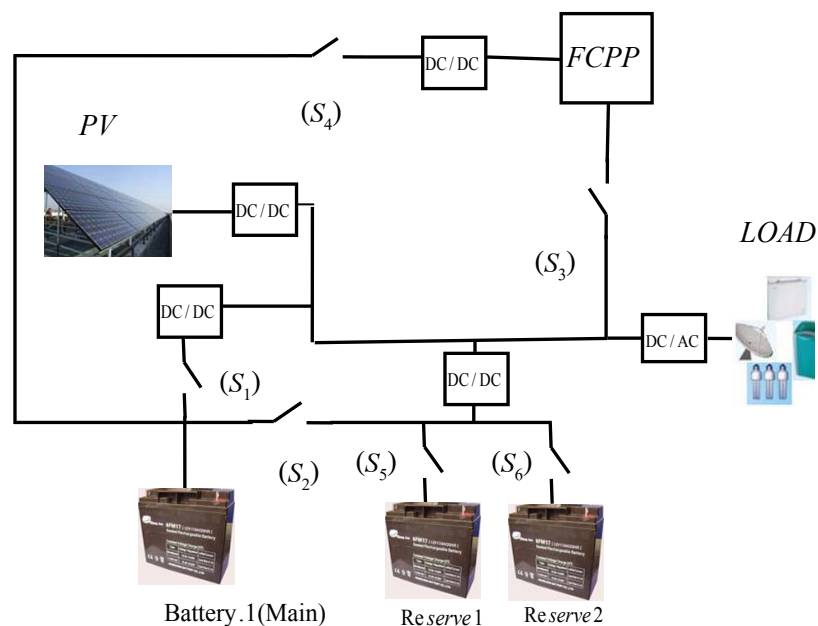


Figure 1 A simple PV/battery system structure.

Real-Time programming of island microgrid PV/battery

The main aim of this system is to satisfy the requirements of the electrical loads qualitatively, while maximizing the utilization of the renewable energy source and optimizing the operation of the battery bank and PV. Therefore, an efficient control strategy for this system is necessary. The developed control strategy must be capable of sensing the continuous variations in electrical loads and variation in power production from PV in order to be able to make fast and correct decisions. A successful operation is only possible through a high quality of interaction throughout the battery bank, PV and Fuel Cell Power Plants (FCPP) (**Figure 1**). Fuel cells are on the cutting edge of future technologies and have the potential to reshape our energy future. They use an electrochemical process to turn hydrogen and oxygen into pollution-free electricity and heat.

Battery unit characteristics

Batteries are one of the most used energy storage technologies available on the market. The energy is stored in the form of electrochemical energy, in a set of multiple cells, connected in series or in parallel or both, in order to obtain the desired voltage and capacity. Each cell consists of 2 conductor electrodes and an electrolyte, placed together in a special, sealed container, and connected to an external source or load. The electrolyte enables the exchange of ions between the two electrodes while the electrons flow through the external circuit.

BESS is a solution based on low-voltage power battery modules, connected in series / parallel in order to achieve the desired electrical characteristics. In practice, the battery storage bank used in the PV/battery system consists of a matrix of identical batteries based on the capacity of the PV array. The ULTRALIFE UBBL 10 lithium battery is chosen to serve as the energy storage in this paper. They are currently one of the most popular types of batteries for portable electronics, with one of the best energy-to-weight ratios, no memory effect, and a slow loss of charge when not in use. Mistreatment may cause Li-ion batteries to explode. Li-ion batteries are growing in popularity for defense, automotive, and aerospace applications, due to their high energy density. The mathematical model of this battery can be built based on [11].

Dozens of identical batteries are connected in series to boost the voltage level of the battery matrix, while multiple battery strings are connected in parallel to increase the working current level of the battery storage system. The rated capacity for ULTRALIFE UBBL 10 lithium-ion battery is 6.8 AH. However the valid capacity depends on the discharge current and ambient temperature during the actual setup. **Table 1** show the valid capacity rates of the battery at different discharge current rates when the ambient temperature is 25 °C. **Table 2** shows the valid capacity rate of the battery at different ambient temperatures when the discharge current is 2 A. All the data is collected from the ULTRALIFE UBBL 10 lithium-ion battery test results [11].

Table 1 Valid capacity rate at different discharge current rates.

Discharge current (A)	Valid capacity rate of the battery
1.0	1.0
3.0	1.0
4.0	0.95
6.0	0.90

Table 2 Valid capacity rate at different ambient temperatures.

Ambient temperature (°C)	Valid capacity rate of the battery
-30	0.75
-20	0.93
25	1.00
50	1.01
60	1.01

Real-time programming algorithm

In this paper, the programming, based on the characteristic rate λ is affected by the discharge current and ambient temperature in practice. We define this relationship in Eq. (1);

$$\lambda = f(i(t), T) \tag{1}$$

where $i(t)$ is the discharge current of the battery bank, and T is the ambient temperature. Taking the derivative on both sides of Eq. (1) will yield [11];

$$\partial\lambda = \frac{\partial f}{\partial i} \partial i + \frac{\partial f}{\partial T} \partial T \tag{2}$$

The corresponding ∂i , ∂T and $\partial\lambda$ can be easily calculated based on the data from **Tables 1** and **2**. Having expressed them in matrix form, we get Eq. (3) [11];

$$\begin{bmatrix} \partial\lambda^1 \\ \vdots \\ \partial\lambda^n \end{bmatrix} = \begin{bmatrix} \partial i^1 & \partial T^1 \\ \vdots & \vdots \\ \partial i^n & \partial T^n \end{bmatrix} \begin{bmatrix} \frac{\partial f}{\partial i} & \frac{\partial f}{\partial T} \end{bmatrix}^T \tag{3}$$

Using the least-square method we obtain the values of $\frac{\partial f}{\partial i}$, $\frac{\partial f}{\partial T}$; then, λ can be obtained as;

$$\lambda = \frac{\partial f}{\partial i} (i - i_{ref}) + \frac{\partial f}{\partial T} (T - T_{ref}) + \lambda_{ref} \tag{4}$$

where the reference values can be chosen from **Tables 1** or **2**. In this paper, $\lambda_{ref} = 1.0$, $T_{ref} = 298$ K (25 °C), and $i_{ref} = 1.0$ A.

The positive direction is defined when the current flows out from the battery. Hence, the charge current is considered as a negative value [12]. Normally, SD (state of discharge) is defined in Eq. (5);

$$SD = \frac{\int_0^t id\tau}{Q} \tag{5}$$

Based on the definition, SD (state of discharge) is 0 at the beginning of discharge and is 1 when the battery is fully discharged. Generally speaking, i is the discharge current of the battery, and Q is the capacity of the battery. If the current i can be negative (charge current), t is the total time that the battery has been used. SD gives an indication of the energy that the battery has used. For example, if the SD is 0.6 after several charging (not fully) and discharging (not fully) cycles, it means that there are still 0.4 units of energy inside the battery. In the real-time programming algorithm, SD must be controlled between 0 and λ , considering the safety of the battery. λ can be calculated using Eq. (1), based on the average discharge current in a short time and the ambient temperature. Here, the average current is used to avoid the effect of a big variation in discharge current. Charging/discharging current must be controlled to meet the requirement of battery safety.

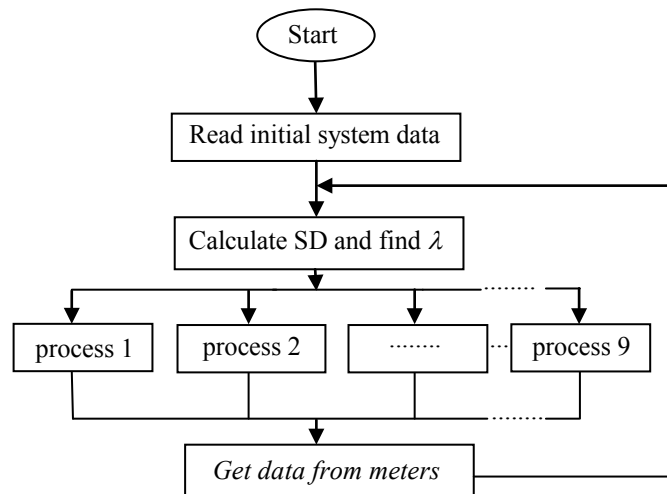


Figure 2 Real-time scheduling flowchart.

To make better use of the battery in the PV/battery system, and control the charging/discharging of the battery in real-time, there are several rules which must be followed:

First, it is assumed reserved batteries are fully discharged, and then, when the produced power of PV is greater than the load, process 1 to 3 will be performed in the following manner:

Process 1: when SD1 is in the range $[0, \lambda]$ and $SD2 = SD3 = 1$, the PV will charge the main battery to make sure the excess power is stored in the main battery. Power is transferred from the PV to the load, as well as from the PV to the main battery.

Process 2: when $SD1 = 0$, $SD2$ is in the range $[0, \lambda]$ and $SD3 = 1$, the extra power from the PV will be sent to the reserved battery1. Power is transferred from the PV to the load, as well as from the PV to the reserved battery1.

Process 3: When $SD1 = SD2 = 0$ and $SD3$ is in the range $[0, \lambda]$, then the extra power of PV will be sent to the reserved battery 2. Power is transferred from the PV to the load as well as from the PV to the reserved battery 2.

When the produced power of PV is less than load, process 4 to 9 will be performed in the following manner:

Process 4: when $SD1$ is in the range $[0, \lambda]$ and $SD2 = SD3 = 1$, the main battery will discharge its energy to the load. Power is transferred from the PV to the load, as well as from the main battery to the load.

Process 5: when $SD1 = 0$ and $SD2 = SD3 = 1$, FCPP transfers power to the load.

Process 6: when $SD1$ is in the range of $[0, \lambda]$ and $SD2 = SD3 = 1$, the main battery will discharge its energy to the load.

Process 7: when $SD1 = SD2 = SD3 = 1$, power is transferred to the load by PV and FCPP.

Process 8: when $SD1$ and $SD3$ are in the range $[0, \lambda]$ and $SD2 = 0$, only reserved battery 2 will discharge its energy to the load.

Process 9: when $SD1 = SD3 = 1$ and $SD2$ is in the range $[0, \lambda]$, only reserved battery 1 will discharge its energy to the load.

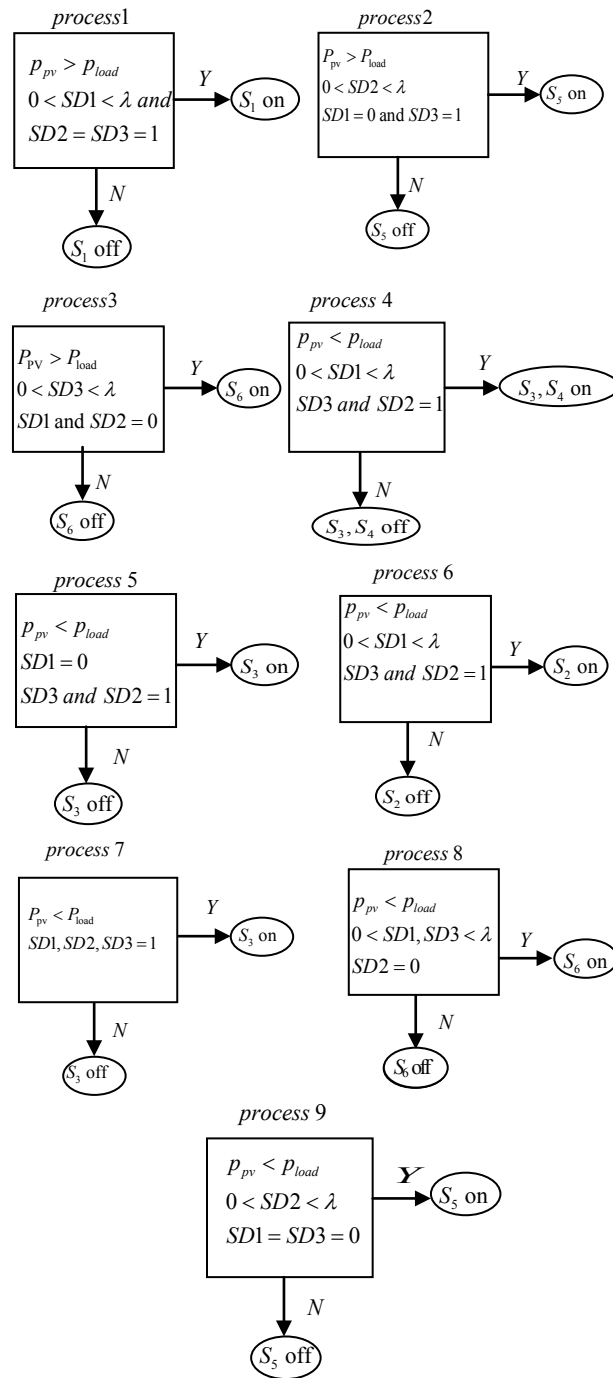


Figure 3 Process flowchart.

Additionally, some economic issues should be considered. The main battery should be charged during off-peak hours, when there is no excess power from the battery, and should be discharged during peak hours if possible. The real-time programming algorithm is shown in the flow chart in **Figures 2** and **3**.

PV array and load

Electricity is generated when photons from sunlight hit electrons and are converted into a higher state of energy in the photovoltaic solar panel. The term “photovoltaic” denotes the unbiased operating mode of a photodiode, in which the current flowing through the device is entirely caused by light energy. A PV array generates electric power by using solar cells packaged in photovoltaic modules, often electrically connected in multiples, to convert energy from the sun into electricity.

A large number of scientific articles have proposed mathematical models of current/voltage terminal characteristics of PV cells and can be used to model the PV cells [13-15]. These papers focus on the power production in the PV array. Because human activities follow certain cycles, most systems supplying energy services to a large population will experience similar cycles. They include the electric power system and PV system. One attractive factor of PV is that generation roughly correlates with peak electricity demand, as shown in **Figure 4** [12,16,17].

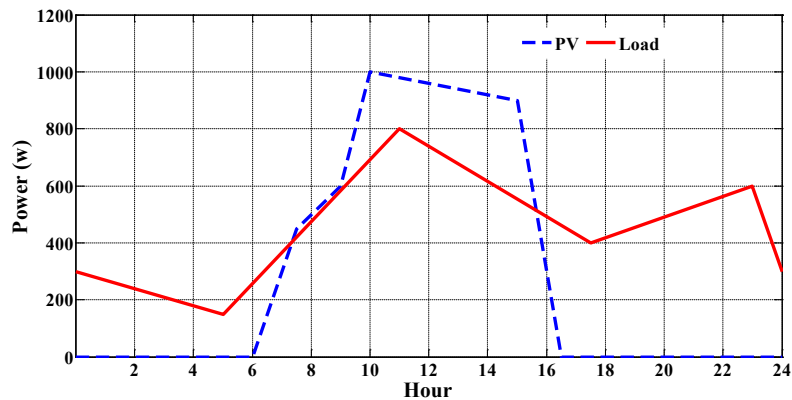


Figure 4 Sample hourly PV generation and System load.

Simulation results

The simulation system is simplified by using the DC power source in place of the AC power source, which does not affect the simulation results. The curve of state of the batteries is depicted in **Figure 5**. The PV/demand curve is the same as the curve in **Figure 4**. This is because the PV and demand module are built based on the data of **Figure 4**. The main battery is charged when the power production from PV is greater than the load demand or during the off-peak hours, and is discharged when the power production from PV is less than the load demand, which can be easily found from **Figure 6**. State of discharge for batteries are kept at 0.95 at the end of the discharge cycle. This is because the discharge current is controlled at 5A in the simulation system. Based on the 5A of discharge current and at normal temperature, λ is found to be 0.95. This is quite reasonable, and closely meets the programming algorithm discussed before.

The switches ($S_1 - S_6$) in the PV/battery simulation system correspond to those of the system shown in **Figure 1**, and the states of switches are shown in **Figure 6**.

Considering **Figures 5** and **6** together, SD1, SD2 and SD3 are equal to 1 at the beginning of the simulation, which means that the main battery is fully discharged and cannot supply system load any more. The power generated by PV is zero at that time.

From **Figure 6**, the state of switch S_3 is 1, which means that it is on, and power is transferred from the FCPP to the load. During 01:00 - 04:00 in the morning, the switch of S_4 is turned on. The main battery is charged at that time, because it is the off-peak time defined in the control scheme in the simulation system. One hour later, the main battery is fully charged (SD1 = 0), and switch S_4 is turned off. At 06:00 to 07:00, the PV starts to generate electricity.

However the power is not enough for the load at that time. The switch S_3 is turned on and S_2 is turned off in **Figure 6**, and power is transferred from the FCPP to the load, as well as from the PV to the load.

One hour later (after 07:00), the power generated by PV is greater than the load. Therefore, the power is transferred from the PV to the load, as well as from the PV to the main battery.

The main battery is fully charged (SD1 = 0) at about 10:05, as shown in **Figure 5**. In the period of time of 10:05 to around 13:00, reserved battery 1 is being charged to receive extra produced power by PV. Afterward, S_6 is turned on and reserved battery 2 starts charging.

Due to the large capacity of reserved batteries, the maximum produced power of PV is less than the total capacity of reserved batteries. Therefore, reserved battery 2 is not fully charged, and it is charged until 15:30. After that, when PV power becomes less than load demand, reserved battery 2, and then 1, start discharging, respectively. When the total reserved power in the batteries is consumed, S_3 is turned on again, and FCPP supports the load.

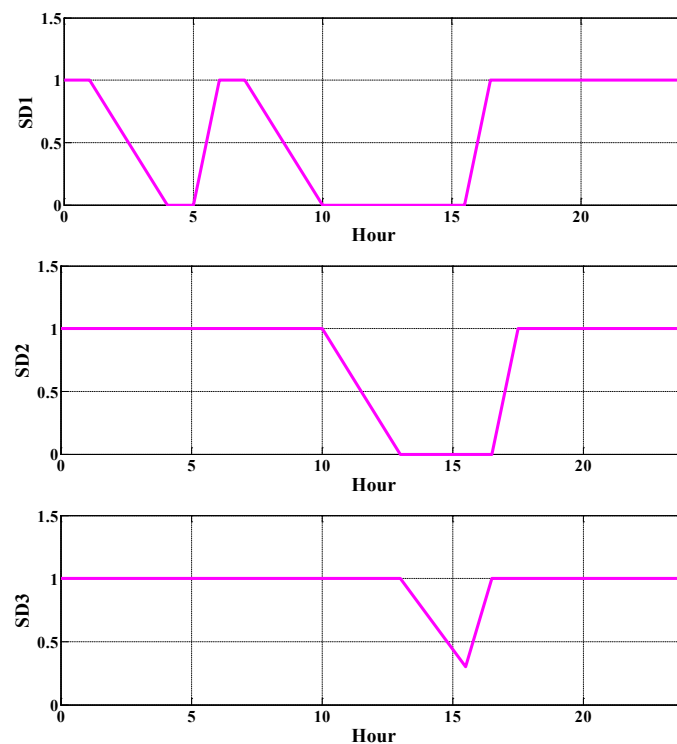


Figure 5 State of the batteries.

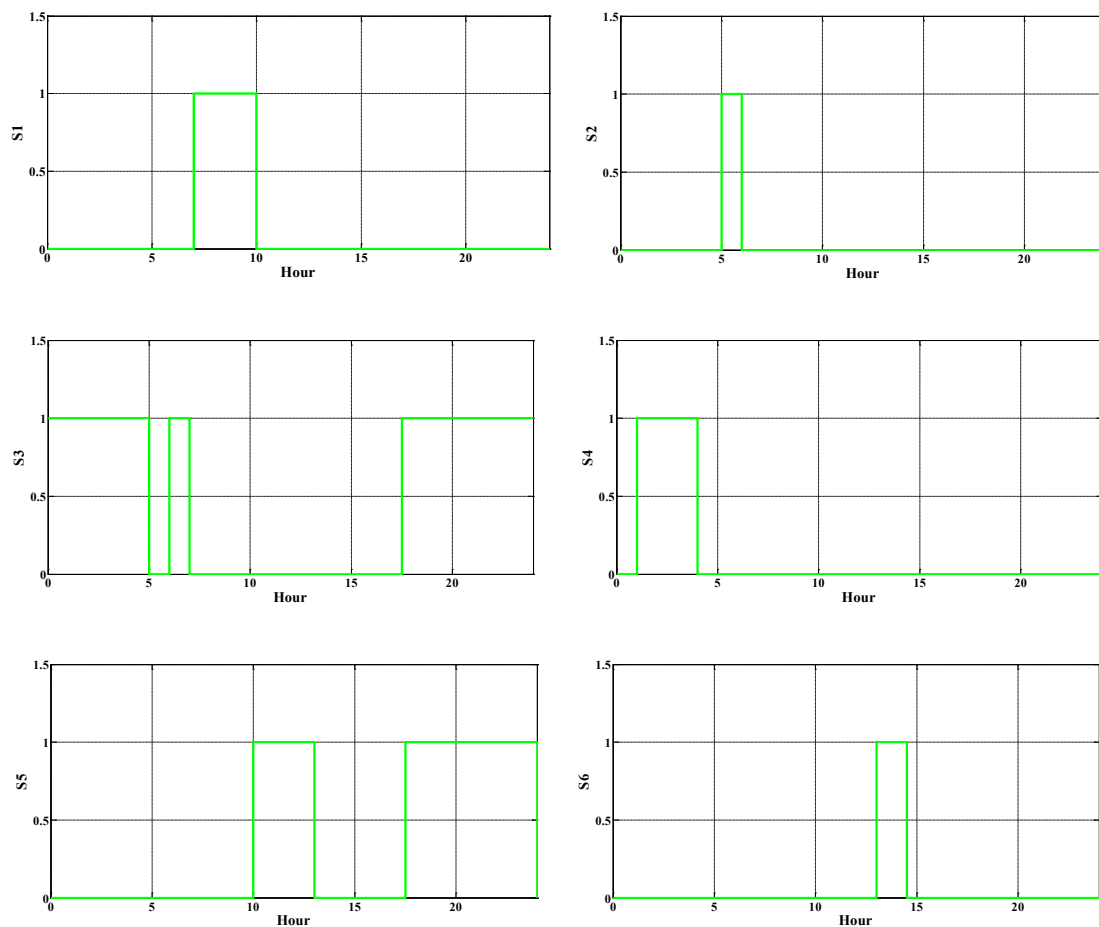


Figure 6 State of switches.

Conclusions

In this paper, a special real-time programming algorithm of ESS in an island MG PV/battery system has been developed. The programming algorithm considers many aspects of battery characteristics that were not considered previously. They include battery charging / discharging characteristics and current and temperature dependence. The results of the 1-day simulation using the scheduling algorithm have been analyzed. The valid capacity rate λ at different discharge currents and ambient temperatures has been discussed in the algorithm, and it ensures that the batteries work in its safe range. The simulation results match with the main design idea of the programming algorithm quite well.

Acknowledgements

The authors gratefully acknowledge the contributions of Mr. Abdollah Khorramdel, Mrs. Robabeh Kargar, and Mrs. Sara Khorramdel, for their technical support on this document.

References

- [1] B Khorramdel and M Raoofat. Optimal stochastic reactive power scheduling in a microgrid considering voltage droop scheme of DGs and uncertainty of wind farms. *J. Eng.* 2012; **45**, 994-1006.
- [2] B Khorramdel, H Khorramdel and H Marzooghi. Multi-objective optimal operation of microgrid with an efficient stochastic algorithm considering uncertainty of wind power. *Int. J. Rev. Mod. Sim.* 2011; **4**, 3079-89.
- [3] L Bo and M Shahidehpour. Short-term scheduling of battery in a grid-connected PV/battery system. *IEEE Trans. Power Syst.* 2005; **20**, 1053-61.
- [4] R Abarghoee, T Niknam, A Roosta, A Malekpour, M Zare. Probabilistic multiobjective windthermal economic emission dispatch based on point estimated method. *J. Eng.* 2012; **37**, 322-35.
- [5] M Shahidehpour. Investing in expansion: The many issues that cloud transmission planning. *IEEE Power Eng.* 2004; **2**, 14-8,
- [6] M Shahidehpour and F Schwatz. Don't let the sun go down on PV. *IEEE Power Eng.* 2004; **2**, 40-8.
- [7] S Basu, L Norum and D Dalal. An improved PV battery charger for low cost low power stand alone low power systems. *In: Proceedings of the International Conference on Sustainable Energy Technology, Singapore, 2008*, p. 1157-60.
- [8] S Wei-Fu, H Shyh-Jier and EL Chin. Economic analysis for demand-side hybrid photovoltaic and battery energy storage system. *IEEE Trans. Indus. Appl.* 2001; **37**, 171-7.
- [9] RL Hammond, JF Turpin, GP Corey, TD Hund and SR Harrington. PV batteries and charge controllers: technical issues, costs, and market trends. *In: Proceedings of the 26th International Conference on Photovoltaic Specialists, USA, 1997*, p. 1165-8.
- [10] M Becherif, D Paire and A Miraoui. Energy management of solar panel and battery system with passive control. *In: Proceedings of the International Conference on Clean Electrical Power, Italy, 2007*, p. 14-9.
- [11] SX Chen, KJ Tseng and SS Choi. Modeling of lithium battery for energy storage system simulation. *In: Proceedings of the International Conference on Power and Energy Engineering, China, 2009*, p. 1-4.
- [12] SX Chen and HB Gooi. Scheduling of energy storage in a grid-connection PV/Battery system via simplorer. *In: Proceedings of the IEEE Conference on Tencon Region, Singapore, 2009*, p. 1-5,
- [13] BYH Lin and R C Jordan. The interrelationship and characteristic distribution of direct, diffuse, and total solar energy, *J. Solar Eng.* 1960; **4**, 1-19.
- [14] DG Erbs, SA Klein and JA Duffie. Estimation of diffuse radiation fraction for hourly, daily, and monthly average global radiation. *J. Solar Eng.* 1982; **28**, 221-302.
- [15] R Perez, R Seals, P Ineichen, R Stewart and D Menicucci. A new simplified version of the Perez diffuse irradiance model for tilted surfaces. *J. Solar Eng.* 1987; **39**, 221-31.
- [16] P Kirawanich and RO Connell. Potential harmonic impact of micoturbines on a commerical power distribution system. *IEEE Power Eng.* 2003; **2**, 1118-23.
- [17] A Fanny and B Dougherty. Building integrated photovoltaic test facility transactions of ASME. *J. Solar Eng.* 2001; **123**,194-9.